JOURNAL OF THERMOPHYSICS AND HEAT TRANSFER
Vol. 25, No. 2, April–June 2011

# Thermomagnetic Convection Around a Hot Circular Cylinder in a Square Cold Enclosure

C. Prax* and H. Sadat*
*Université de Poitiers, F86022 Poitiers, France*

DOI: 10.2514/1.50639

**Magnetic convection of air around a hot circular cylinder placed in a square cavity under the influence of an external magnetic field and in absence of gravity is considered. Fluid motion occurs due to the gradients of the magnetic and temperature fields. A collocation meshless method is used for the numerical solution of the governing equations. The results are presented through temperature contours and velocity vectors at steady state. Nusselt numbers are also given for magnetic Rayleigh numbers of $10^5$ and $10^6$.**

## I. Introduction

NATURAL convection in an enclosure with hot bodies embedded within it is relevant to many applications such as heat exchangers and cooling of electronic equipments. This problem is therefore receiving increasing attention. Kumar and Dalal [1] numerically studied two-dimensional natural convection around a square, horizontal, heated cylinder placed inside an enclosure up to Rayleigh number $Ra = 10^6$. Asan [2] has considered the case of two-dimensional natural convection in an annulus between two isothermal concentric square ducts. Moukalled and Acharya [3] and Shu and Zhu [4] have carried out a series of numerical studies on natural convection between high temperature inner circular cylinder and a low temperature outer square enclosure and for three different aspect ratios. This geometry has been considered numerically by Yoon et al. [5] for a Rayleigh number $Ra = 10^7$. They investigated the effect of the inner cylinder location on the heat transfer and fluid flow and found two critical positions as lower and upper bounds within which the flow is steady. Angeli et al. [6] have investigated numerically the buoyancy flow regimes for this geometrical case. They have particularly discussed the occurrence of time dependant behavior.

It is well established that there exist external forces that can influence natural convection. Magnetic force for example can be induced in electrically conducting or nonconducting fluids. In the case of paramagnetic fluids, the variation of their magnetic susceptibility with temperature plays a key role. One such a fluid is air which is composed by paramagnetic oxygen (with a magnetic susceptibility at ambient temperature equal to $1.91\ 10^{-6}$) and diamagnetic nitrogen (with a magnetic susceptibility equal to $-6.8\ 10^{-9}$). The total magnetic susceptibility of air is the summation of the magnetic susceptibilities of air constituents weighted by their partial pressure or concentration. Because the magnetic susceptibility of nitrogen is very small, its contribution on the total magnetic susceptibility is negligible. Therefore, the magnetic susceptibility of air is mainly determined by oxygen concentration. One of the first applications of this phenomenon can be found in the development of paramagnetic oxygen sensors which have proven to be very selective and stable [7–9]. Another application can be found in controlling or even generating fluid motions. Indeed, through the temperature-dependence of magnetic susceptibility the thermal gradient renders an internal magnetic field gradient working as a driving force. Finlayson [10] was the first to study theoretically the magnetic convection instability in a presence of homogeneous vertical magnetic field. One of the first experimental works in this field was carried out by Braithwaite et al. [11] who reported enhancement or cancellation of convection in a solution of gadolinium nitrate. Since then many studies have been undertaken both experimentally and numerically [12–16]. Tagawa et al. [17] have presented a model for thermomagnetic convection and carried out numerical simulations in a cubic cavity. Qi et al. [18] and Wakayama [19] have reported very interesting results and applications. Yang et al. [20] and Bednarz et al. [21] have studied the effect of a gradient magnetic field on convection of air in a cavity with a four-pole electric magnet. Bednarz et al. [21–24] have shown both numerically and experimentally how to enhance or suppress heat transfer by the application of a magnetic field and have considered the influence of the positioning of the magnet device.

So far, the majority of previous works were carried out on cavities filled by the magnetic fluid. Yamaguchi et al. [25] have studied experimentally and numerically thermomagnetic convection of a magnetic fluid in a cubic cavity with a heat-generating square cylinder inside under a uniform magnetic field. They used a magnetic fluid which has a strong temperature dependence of the magnetic magnetization in the room temperature range. The top and bottom walls of their cavity were kept at a constant temperature while the other lateral walls were considered to be adiabatic. They have shown that heat transfer is enhanced when the magnetic field is present, and that this enhancement diminishes when the relative size of the heating object increases.

To the best of our knowledge, the case of magnetic convection in air in a cavity with a heat-generating object inside has not been reported. As an initial stage, the main goal of this paper is therefore to study numerically 2-D thermomagnetic convection in air when a circular cylinder is placed in the cavity. Because of the large number of parameters governing the problem, we shall restrict ourselves (in this preliminary work) to the case where gravity is not present. The second objective of this work is to show that a meshless numerical method can be used to solve the problem as the previous numerical studies have used finite difference, finite volume, or finite element methods. This paper is organized as follows: in Secs. II and III, the physical system and governing equations are first presented. Then, the meshless method based numerical code used to solve the problem is validated on the case of pure natural convection in Sec. IV where numerical results of magnetic convection are also presented and discussed.

## II. Physical System

A hot cylinder of radius $r$, of temperature $T_H$, is placed at the center of a square enclosure whose walls are maintained at temperature $T_C (T_H > T_C)$. The cavity is positioned in the air gap of two magnet

Received 5 May 2010; revision received 17 December 2010; accepted for publication 22 December 2010. 

*Institut PPRIME, Centre National de la Recherche Scientifique, Université de Poitiers, ENSMA, Département Fluides, Thermique, Combustion, ESIP, 40, avenue du recteur Pineau.

bars face to face so that the fluid is submitted to a gradient of magnetic field. The fluid is assumed Newtonian while viscous dissipation effects are negligible and the flow is laminar and steady. The dimension of both cylinder and enclosure along the third direction is supposed to be sufficiently long (as compared with the square section side) to allow the end effects to be neglected. Under this condition, as it has been observed in [26] where natural convection in a cavity with a heat source has been experimentally studied, the problem can be considered from a two-dimensional point of view. The magnets have square sections of the same size as the cavity walls and the solid walls of the cavity are supposed to have no influence on the magnetic field. By considering both the symmetry of the boundary conditions and the symmetry of the magnetic field, the study is limited to the midplane containing the axis of the magnet device (Fig. 1). The center of the enclosure is taken as the origin of the coordinate system $(x, y)$.

The magnets are parallel to the vertical walls and the distance $d$ to the walls is fixed to $0.1L$ in all the following simulations. The axis of the magnet device is identified by $y = y_m$ and the central point of the magnet faces is located at the coordinate $(x = (L/2 + d), y_m)$. Three different aspect ratios ($R = L/2r = 5$, 2.5, and 1.67) are considered.

An analytic solution given by Manikonda and Berz [27] is used to compute the magnetic field in the air-gap of magnetized bars. Figure 2 shows in its left half part the resulting shapes of the normalized magnetic flux density $B^+ = \frac{B}{B_{\max}}$ inside the cavity and the gradient of the squared magnetic induction in its right half part. There is symmetry about the axial line of magnets and over the vertical midline.

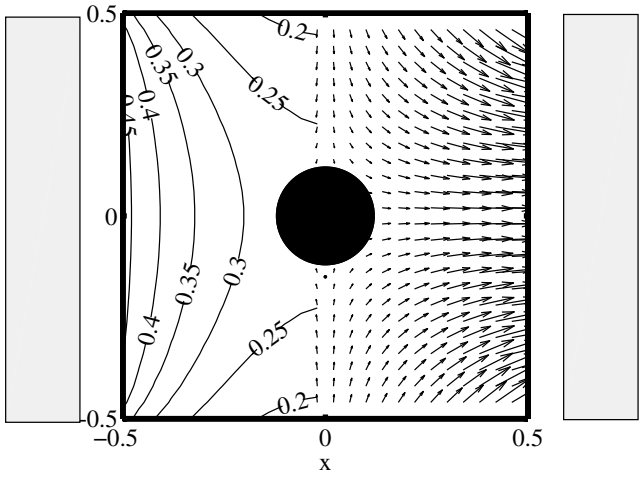


**Fig. 2 Amplitude of $B^+$ (left side) and gradient of the squared magnetic induction in the cavity (right side) when the magnets are positioned at $y_m = -0.5$.**

## III. Governing Equations and Solution Procedure

We consider air as a paramagnetic fluid whose magnetic susceptibility is positive and variable with temperature $T$ according to Curie's law [11–14]:

$$\chi(T) = \frac{C}{T} = \frac{\chi_{\text{ref}} T_{\text{ref}}}{T} \tag{1}$$

Reference value $\chi_{\text{ref}}$ of magnetic susceptibility is taken at the ambient reference temperature, $T_{\text{ref}} = 293$ K. Under the effect of the applied magnetic field, the magnetic Kelvin force generated in the fluid writes:

$$\mathbf{f} = \rho \frac{\chi(T)}{2\mu_0} \nabla B^2 \tag{2}$$

where $\mu_0$ is the magnetic permeability of the empty space, $\rho$ the density, and $B$ the magnetic induction vector. This force is small under ordinary conditions unless very strong magnets are used (superconductive magnets, for example). In the absence of gravity such as in microgravity environment, however, it can be significant. Temperature gradients cause convection because susceptibility depends explicitly on density and on temperature.

Since density changes are small, the Boussinesq approximation can be made and by noting that $\frac{\partial \chi}{\partial T} = -\frac{\chi}{T}$, one can show that the magnetic force writes:

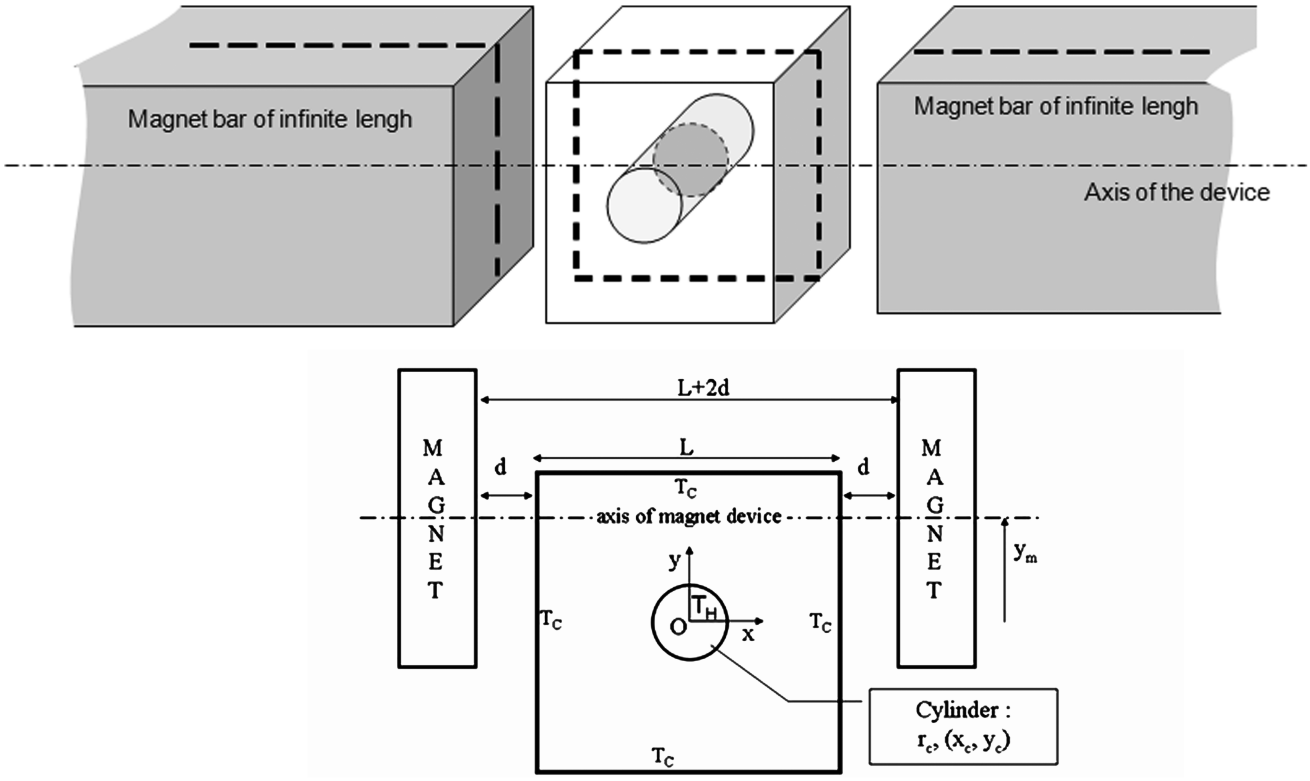


**Fig. 1 Problem layout: a) with the 2-D domain of calculation (in dashed lines), and b) 2-D studied domain.**

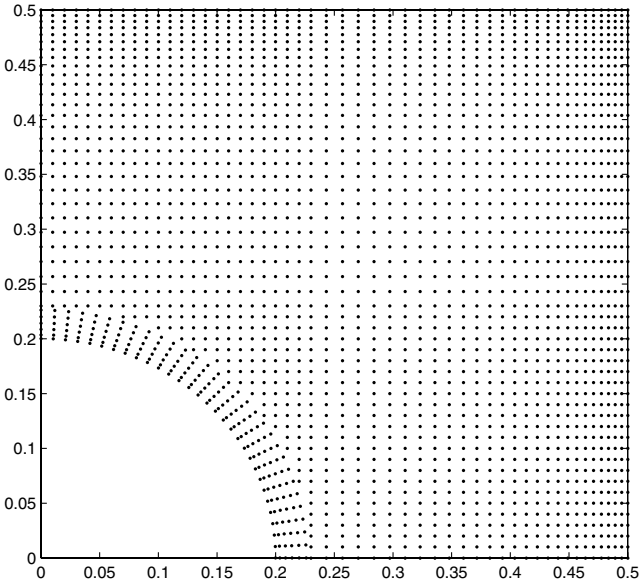


**Fig. 3 Example of refined grid on a quarter of studied domain.**

$$\pi_m = -(T - T_0)\beta\rho_0 \frac{\chi_0 B \nabla B}{\mu_0} \tag{3}$$

This expression can be compared with the classical buoyancy term obtained when dealing with natural convection:

$$\pi_g = (T - T_0) g \beta \rho_0 \tag{4}$$

Equations (3) and (4) show that magnetic convection is similar to natural convection but with an equivalent magnetic gravity: $g_m = \frac{\chi_0 B \nabla B}{\mu_0}$. The direction of this equivalent magnetic gravity is given by the gradient of the squared magnitude of the magnetic field. As a consequence, its direction and magnitude can vary with position.

By using the equivalent magnetic gravity instead of the gravity in the Rayleigh number: $Ra = \frac{g\beta\Delta TL^3}{\nu\alpha}$, one obtains an equivalent local magnetic Rayleigh number: $Ra_m = \frac{\chi_0 B \nabla B \beta \Delta T L^3}{\mu \nu \alpha}$. By using now the maximum value $B_{\max}$ of magnetic induction and by scaling $\nabla B$ by $B_{\max}/L$, one finally obtains the following constant magnetic Rayleigh number: $Ra_m = \frac{\chi_0 B_{\max}^2 \beta \Delta T L^2}{\mu \nu \alpha}$. This expression is equivalent to the product $\gamma Ra$ used by [17] and to the $G$ number used by [14].

We can now write down the Navier–Stokes, continuity and energy equations in the form:

$$\frac{\mathrm{D}\mathbf{V}^+}{\mathrm{D}t^+} = -\nabla P^+ + Pr\nabla^2\mathbf{V}^+ - Ra_m\theta\nabla B^{+2} \tag{5}$$

$$\nabla.\mathbf{V} = 0 \tag{6}$$

$$\frac{\mathrm{D}\theta}{\mathrm{D}t^+} = \nabla^2\theta \tag{7}$$

where $\frac{\mathrm{D}}{\mathrm{D}t}$ is the particular derivative and where the following adimensional variables are introduced:

$$\mathbf{X}^+ = \frac{\mathbf{X}}{L}; \qquad \mathbf{V}^+ = \frac{\mathbf{V}}{U_{\mathrm{ref}}}; \qquad U_{\mathrm{ref}} = \frac{\alpha}{L}; \qquad P^+ = \frac{P}{\rho U_{\mathrm{ref}}^2}$$

$$B^+ = \frac{B}{B_{\max}} \quad t^+ = \frac{t \cdot U_{\mathrm{ref}}}{L}; \qquad \theta = \frac{T - T_0}{\Delta T} \qquad Pr = \frac{\nu}{\alpha}$$

$$Ra_m = \frac{\chi_{\mathrm{ref}} L^2 \beta \Delta T B_{\max}^2}{\mu_0 \nu \alpha}$$

$Pr$ is the Prandtl number and $Ra_m$ is the equivalent magnetic Rayleigh number which quantifies the strength of the magnetic force. $L$ is a characteristic dimension, $\nu$ the kinematic viscosity, $\rho$ the fluid density, $T_0$ a reference temperature, and $\Delta T$ the temperature difference in the domain.

These equations are solved by using a diffuse approximate meshless method together with a projection algorithm for the velocity-pressure coupling which has proved to be accurate for

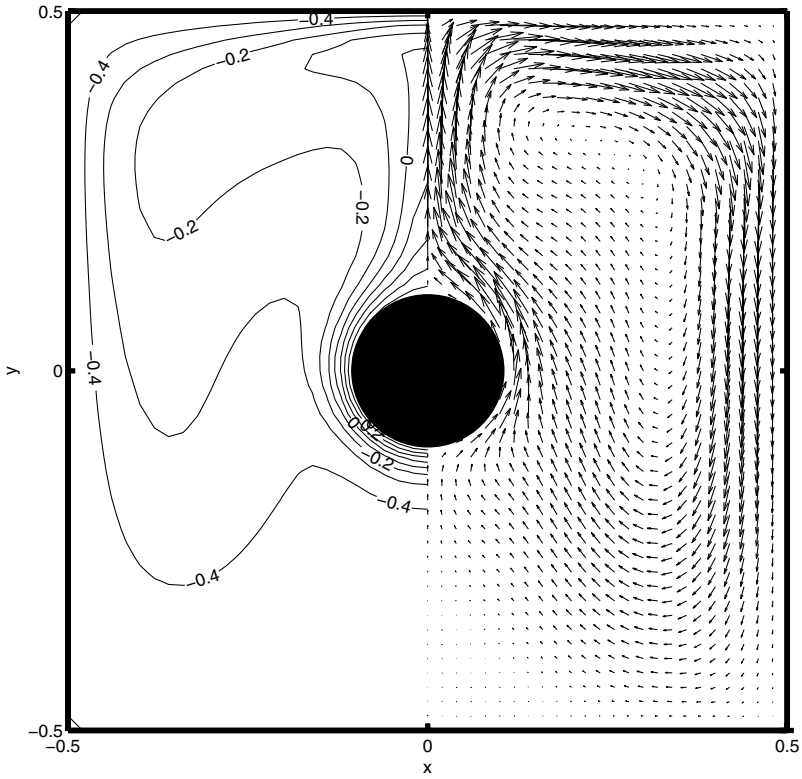


**Fig. 4 Velocity field and isotherms (Natural convection) for $R = 5$ and $Ra = 10^6$ and $y_m = 0$.**

**Table 1 Nusselt numbers and maximum streamfunction value for natural convection**

| | Ra | Nu | | | $\Psi_{max}$ | | |
|---|---|---|---|---|---|---|---|
| | | $R = 5$ | $R = 2.5$ | $R = 1.67$ | $rr = 5$ | $rr = 2.5$ | $rr = 1.67$ |
| Present | 0 | 3.73 | 6.33 | 10.72 | | | |
| Angeli et al [6] | | 3.73 | 6.33 | 10.72 | | | |
| Present | $10^5$ | 7.52 | 9.76 | 12.35 | 10.14 | 8.33 | 5.07 |
| Shu and Zhu [4] | | 7.58 | 9.72 | 12.42 | 9.93 | 8.10 | 5.10 |
| Moukalled and Acharia [3] | | 7.65 | 10.16 | 12.424 | 10.15 | 8.38 | 5.10 |
| Present | $10^6$ | 12.11 | 17.72 | 23.69 | 20.97 | 24.16 | 20.19 |
| Shu and Zhu [4] | | 12.22 | 17.80 | 24.00 | 20.98 | 24.13 | 20.46 |
| Moukalled and Acharia [3] | | 12.214 | 18.748 | 23.24 | 25.35 | 24.07 | 21.30 |

solving both steady and unsteady fluid flow problems. The details of the numerical method can be found in previous works [28–32]. Velocity components are set to zero along the inner and outer cylinder walls. The temperature is set to 0.5 along the inner cylinder and to −0.5 on the outer square enclosure. Once the steady state temperature field has been obtained, the average Nusselt number at a boundary is calculated by the relation:

$$\overline{Nu} = \int_S \frac{\partial \theta}{\partial n}\, \mathrm{d}S$$

where $S$ is the length of the inner or outer surface and $n$ is the outward unit normal vector. At steady state, the Nusselt numbers are the same along the inner and outer cylinder surfaces.

## IV. Results and Discussion

To provide sufficiently accurate solutions, the numerical domain is discretized with $N^*N$ irregular grid, which is refined near the walls of the enclosure and in an annular area around the inner cylinder as shown on Fig. 3 for the quarter of the studied domain. It is worth noting that a mesh sensitivity study has been carried out and has shown that the 101*101 irregular discretization is of sufficient accuracy for all the numerical simulations presented hereafter. For example we found a Nusselt number equal to 12.44, 12.51, and 12.5 for 51*51, 71*71, and 101*101 grids, respectively, for a magnetic Rayleigh number of $10^6$. This 101*101 discretization results in 10036 nodes, 9272, and 7860 nodes for $R = 5$, 2.5, and 1.67, respectively. The projection algorithm has been used to deal with the pressure-velocity coupling. The time step has been monitored although steady state was thought. Its value was set to $10^{-2}$ for $Ra = 10^5$ and $10^{-4}$ for $Ra = 10^6$. Any time step under these values leads to the same solution. A convergence criterion of 0.01% or less change in all nodal values has been selected to check convergence. The mass conservation was also monitored.

### A. Laminar Natural Convection

To validate the computer code developed for this study, a series of calculations has been performed to study the natural convection problem in the absence of magnetic field in the case of an inner cylinder with an aspect ratio $R = 5$. This buoyancy driven convection was studied in [1–5]. The conductive regime is computed first and an average Nusselt number of 2.728 was found. The structure of the flow in the convective regime includes an up-going warm flow due to buoyancy and down-going cold flow at outer regions near the walls. The velocity field and isotherms solutions are presented in Fig. 4 for an aspect ratio of $R = 5$ and for a Rayleigh number of $10^6$.

The mean Nusselt number is 12.11 and the maximum absolute value of velocity is 291.23 at the position on the vertical axis given by the coordinates ($x = 0$, $y = 0.31$).

In Table 1, we present the calculated Nusselt numbers and the maximum values of the streamfunction for two Rayleigh numbers together with the numerical results of Moukalled and Acharya [3], who used a body-fitted finite volume method, and those of Shu and Zhu [4], who used a differential quadrature method. We have also reported the result obtained by [6] in the case of pure heat conduction. It can be seen that our results are comparable in accuracy (relative error less than 1%).

### B. Thermomagnetic Convection

We now turn to the presentation of some results obtained when gravity is not acting and when the magnetic field is present. The typical flow patterns are shown on Fig. 5, where isotherms and velocity vectors are presented for two values of the magnetic Rayleigh number, namely $Ra_m = 10^5$ and $Ra_m = 10^6$ and for an aspect ratio $R = 5$. It can be seen that the flow is symmetrical about the vertical line through the center of the circular cylinder and about the axis of the magnets. The fluid moves up and down along the inner heated cylinder, reaches top and bottom walls of the enclosure, and then moves horizontally outwards and goes down along the vertical walls till the midheight of the cavity. Four eddies are formed symmetrically in the cavity. As the magnetic Rayleigh number increases from $10^5$ to $10^6$, the flow becomes stronger and the eddies

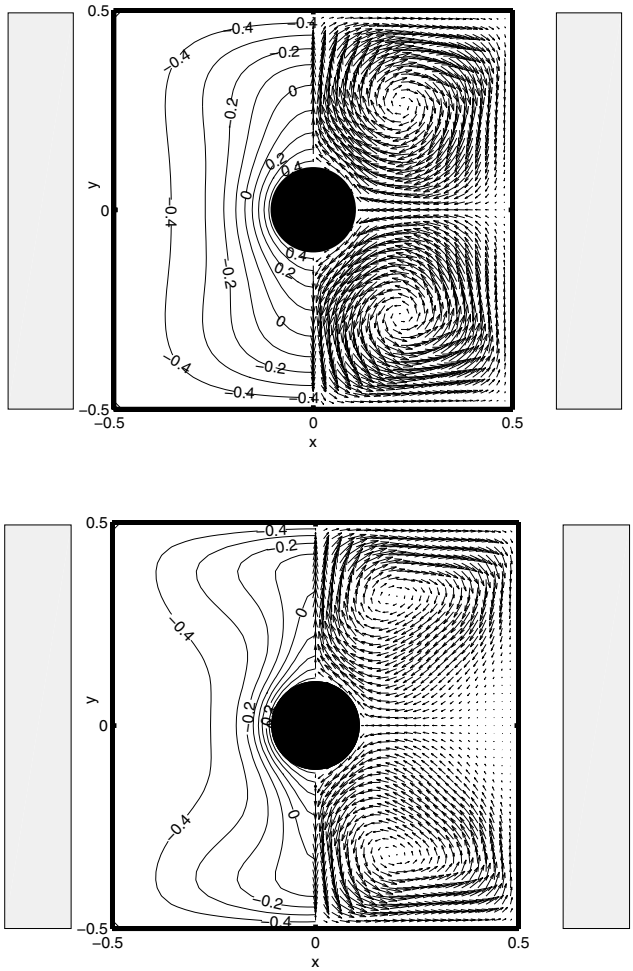


**Fig. 5 Isotherms and velocity vectors for a) $R = 5$ and $Ra_m = 10^5$, and b) $Ra_m = 10^6$.**

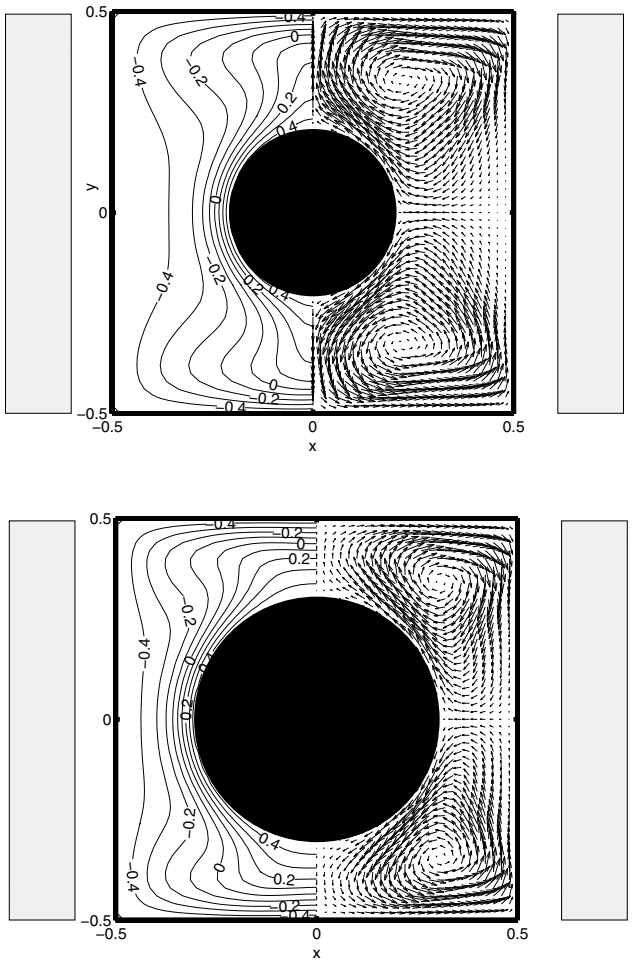


**Fig. 6 Thermal and velocity fields for aspect ratio of $R = 2.5$ and $R = 1.67$ and for $Ra_m = 10^6$.**

move slightly towards the vertical centerline. We can also notice that two symmetrical plumes are developing on top and bottom of the inner cylinder. At $Ra_m = 10^6$, a stagnant zone appears near the vertical walls and at midheight. It is worth to mention that the situation with $Ra_m = 10^6$ can correspond for example to a 20 cm square cavity filled with air at 300 K combined with wall temperature difference of about 19 K and with neodynium magnets of 1.25 Tesla. In these operating conditions, the magnitude of the velocity reaches approximately 1 cm/s.

Similar trends are observed when the aspect ratio is set to $R = 2.5$ and $R = 1.67$. We therefore just present in Fig. 6 the velocity and thermal fields for a magnetic number of $10^6$. It can be seen that for the particular case ($R = 1.67$), the fluid is stagnant in the top and bottom of the cylinder leading to a thermal stratification (similar to conductive regime) [3].

We have gathered in Table 2 the maximum value of the adimensional velocity $|V^+|$ and the global Nusselt numbers. As expected, Nusselt number increases with the magnetic Rayleigh number. It increases also when the aspect ratio is diminishing.

The local Nusselt number along the cylinder as a function of the angular position in radians for the two magnetic Rayleigh numbers is presented in Fig. 7. The maximum values are obtained when $\theta = 0$

**Table 2 Maximum value of adimensional velocity and mean Nusselt number**

| | $R = 5$ | | $R = 2.5$ | | $R = 1.67$ | |
|---|---|---|---|---|---|---|
| | $\|V^+\|$ | $Nu$ | $\|V^+\|$ | $Nu$ | $\|V^+\|$ | $Nu$ |
| $Ra_m = 10^5$ | 14.86 | 4.68 | 17.79 | 7.40 | 17 | 11.24 |
| $Ra_m = 10^6$ | 61.68 | 7.58 | 66.35 | 12.50 | 81.59 | 16.23 |

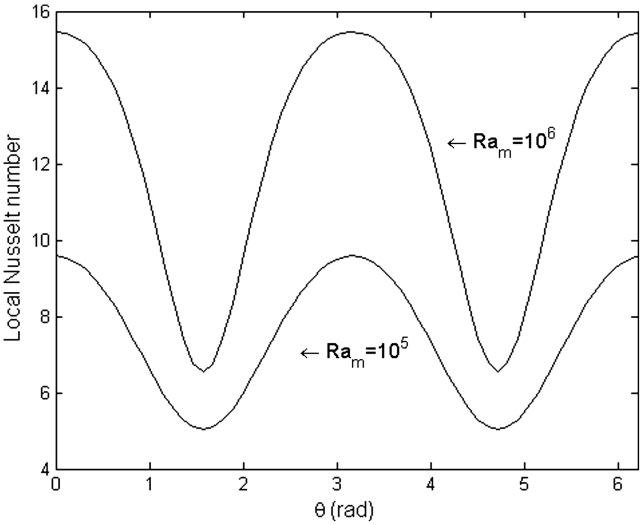


**Fig. 7 Local Nusselt number along the inner cylinder ($R = 2.5$).**

and $\theta = \pi$, corresponding to the thin boundary layers that are developing at that positions. On the other hand, minimum local Nusselt numbers are found on the top and bottom of the inner cylinder.

Finally, let us have a look at the situation where the magnets are shifted downward as shown in Fig. 8 (where the normalized magnetic

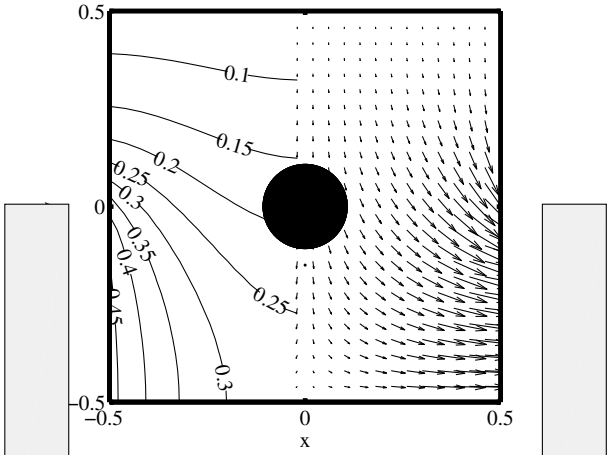


**Fig. 8 Amplitude of $B^+$ (left side) and gradient of the squared magnetic induction between the magnets (right side).**

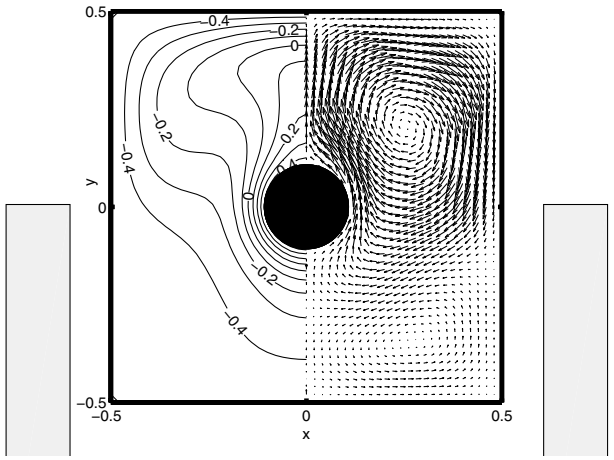


**Fig. 9 Velocity vectors and isotherms when the magnets are positioned at $y_m = -0.5$ for $Ra_m = 10^6$.**

flux density and the gradient of the squared magnetic induction are also presented). In this situation, one can observe in Fig. 9 that the cold fluid moves downward along the vertical walls while hot fluid plume rises at the top of the hot inner cylinder. This is due to the great value of the magnetic force near the edges of the magnets and to the fact that these forces attract the fluid downward, while at the same time in the bottom of the cavity the fluid is attracted toward the vertical walls. Further, at the two lower corners of the cavity, the temperature is almost uniform and there is practically no driving magnetic force. Consequently, the fluid hardly flows and is badly stirred. Therefore, the global pattern consists in two cells located at an angle of 45° approximately. The isotherms show that a plume is developing and moves in the direction opposite to the magnets.

## V. Conclusions

In this article, numerical calculations are carried out for magnetic convection induced by a temperature difference between a cold outer square enclosure and a hot inner circular cylinder in absence of gravity. A meshless method has been used and results are presented for magnetic Rayleigh numbers $Ra = 10^5$ and $Ra = 10^6$. The flow patterns and heat transfer characteristics are presented for three different aspect ratios. It has been shown that thermomagnetic convection can find applications, particularly in miniature cooling devices for electronics and low-gravity environments where natural convection fails to provide adequate heat transfer.

## References


[1] Kumar De, A., and Dalal, A., "A Numerical Study of Natural Convection Around a Square, Horizontal, Heated Cylinder Placed in an Enclosure," *International Journal of Heat and Mass Transfer*, Vol. 49, Nos. 23–24, 2006, pp. 4608–4623. doi:10.1016/j.ijheatmasstransfer.2006.04.020

[2] Asan, H., "Natural Convection in an Annulus Between Two Isothermal Concentric Square Ducts," *International Communications in Heat and Mass Transfer*, Vol. 27, No. 3, 2000, p. 367. doi:10.1016/S0735-1933(00)00117-2

[3] Moukalled, F., and Acharya, S., "Natural Convection in the Annulus Between Concentric Horizontal Circular and Square Cylinders," *Journal of Thermophysics and Heat Transfer*, Vol. 10, No. 3, 1996, pp. 524–531. doi:10.2514/3.820

[4] Shu, C., and Zhu, Y. D., "Efficient Computation of Natural Convection in a Concentric Annulus Between an Outer Square Cylinder and an Inner Circular Cylinder," *International Journal for Numerical Methods in Fluids*, Vol. 38, No. 5, 2002, pp. 429–445.

[5] Yoon, H. S., Ha, M. Y., Kim, B. S., and Yu, D. H., "Effect of the Position of a Circular Cylinder in a Square Enclosure on Natural Convection at Rayleigh Number of 107," *Physics of Fluids*, Vol. 21, No. 4, 2009, p. 047101. doi:10.1063/1.3112735

[6] Angeli, D., Levoni, P., and Barozzi, G. S., "Numerical Predictions for Stable Buoyant Regimes Within a Squarecavity Containing a Heated Horizontal Cylinder," *International Journal of Heat and Mass Transfer*, Vol. 51, Nos. 3–4, 2008, pp. 553–565. doi:10.1016/j.ijheatmasstransfer.2007.05.007

[7] Schmid, U., Seidel, H., Mueller, G., and Becker, T., "Theoretical Considerations on the Design of a Miniaturised Paramagnetic Oxygen Sensor," *Sensors and Actuators B: Chemical*, Vol. 116, Nos. 1–2, July 2006, pp. 213–220. doi:10.1016/j.snb.2005.11.080

[8] Kovacich, R. P., Martin, N. A., Clift, M. G., Stocks, C., Gaskin, I., and Hobby, J., "Highly Accurate Measurement of Oxygen Using a Paramagnetic Gas Sensor," *Measurement Science and Technology*, Vol. 17, No. 6, 2006, pp. 1579–1585. doi:10.1088/0957-0233/17/6/040

[9] Lee, J.-H., Tsai, C.-L., Fann, C.-S., and Wang, S.-H., "Design of an Acousto-Magnetic Oxygen Sensor," *Journal of Medical and Biological Engineering*, Vol. 22, No. 4, 2002, pp. 193–198.

[10] Finlayson, B. A., "Convective Instability of Ferromagnetic Fluids," *Journal of Fluid Mechanics*, Vol. 40, No. 04, 2006, pp. 753–767. doi:10.1017/S0022112070000423

[11] Braithwaite, D., Beaugnon, E., and Tournier, R., "Magnetically Controlled Convection in a Paramagnetic Fluid," *Nature*, Vol. 354, No. 6349, 1991 pp. 134–136. doi:10.1038/354134a0

[12] Khaldi, F., and Gillon, P., "Experimental and Numerical Investigation of Thermomagnetic Convection in a Non Electroconducting Fluid, *Comptes Rendus Hebdomadaires des Seances de l'Academie des Sciences, Serie B: Sciences Physiques*, Vol. 329, No. 5, 2001, pp. 357–362. doi:10.1016/S1620-7742(01)01339-3

[13] Khaldi, F., Noudem, J., and Gillon, P., "On the Similarity Between Gravity and Magneto-Gravity Convection Within a Non-Electro-conducting Fluid in a Differentially Heated Rectangular Cavity," *International Journal of Heat and Mass Transfer*, Vol. 48, No. 7, 2005, pp. 1350–1360. doi:10.1016/j.ijheatmasstransfer.2004.10.007

[14] Sophy, T., Sadat, H., and Gbahoué, L., "Convection Thermo-magnétique dans une Cavité Différentiellement Chauffée," *International Communications in Heat and Mass Transfer*, Vol. 32, No. 7, July 2005, pp. 923–930. doi:10.1016/j.icheatmasstransfer.2004.10.026

[15] Mukhopadhyay, A., Ganguly, R., Sen, S., and Puri, I., "A Scaling Analysis to Characterize Thermomagnetic Convection," *International Journal of Heat and Mass Transfer*, Vol. 48, No. 17, 2005, pp. 3485–3492. doi:10.1016/j.ijheatmasstransfer.2005.03.021

[16] Krakov, M. S., and Nikiforov, I. V., "To the Influence of Uniform Magnetic Field on Thermomagnetic Convection in Square Cavity," *Journal of Magnetism and Magnetic Materials*, Vol. 252, Nov. 2002, pp. 209–211. doi:10.1016/S0304-8853(02)00653-4

[17] Tagawa, T., Shigemitsu, R., and Ozoe, H., "Magnetizing Force Modelled and Numerically Solved for Natural Convection of Air in a Cubic Enclosure: Effect of the Direction of the Magnetic Field," *International Journal of Heat and Mass Transfer*, Vol. 45, No. 2, Jan. 2002, pp. 267–277. doi:10.1016/S0017-9310(01)00149-1

[18] Qi, J., Wakayama, N. I., and Yabe, A., "Attenuation of Natural Convection by Magnetic Force in Electro-Nonconducting Fluids," *Journal of Crystal Growth*, Vol. 204, No. 3, 1999, pp. 408–412. doi:10.1016/S0022-0248(99)00218-3

[19] Wakayama, N. I., "Magnetic Promotion of Combustion in Diffusion Flames," *Combustion and Flame*, Vol. 93, No. 3, 1993, pp. 207–214. doi:10.1016/0010-2180(93)90103-A

[20] Yang, L., Ren, J., Song, Y., and Guo, Z., "Free Convection of a Gas Induced by a Magnetic Quadrupole Field," *Journal of Magnetism and Magnetic Materials*, Vol. 261, No. 3, May 2003, pp. 377–384. doi:10.1016/S0304-8853(02)01487-7

[21] Bednarz, T., Lei, C., Patterson, J. C., and Ozoe, H., "Effects of a Transverse, Horizontal Magnetic Field on Natural Convection of a Paramagnetic Fluid in a Cube," *International Journal of Thermal Sciences*, Vol. 48, No. 1, 2009, pp. 26–33. doi:10.1016/j.ijthermalsci.2008.03.011

[22] Bednarz, T., Patterson, J. C., Lei, C., and Ozoe, H., "Enhancing Natural Convection in a Cube Using a Strong Magnetic Field: Experimental Heat Transfer Rate Measurements and Flow Visualization," *International Communications in Heat and Mass Transfer*, Vol. 36, No. 8, 2009, pp. 781–786. doi:10.1016/j.icheatmasstransfer.2009.06.005

[23] Bednarz, T., Fornalik, E., Ozoe, H., Szmyd, J. S., Patterson, J. C., and Lei, C., "Influence of a Horizontal Magnetic Field on the Natural Convection of Paramagnetic Fluid in a Cube Heated and Cooled from Two Vertical Side Walls," *International Journal of Thermal Sciences*, Vol. 47, No. 6, June 2008, pp. 668–679. doi:10.1016/j.ijthermalsci.2007.06.019

[24] Bednarz, T., Tagawa, T., Kaneda, M., Ozoe, H., and Szmyd, S., "Convection of Air in a Cubic Enclosure with an Electric Coil Inclined in General Orientations," *Fluid Dynamics Research*, Vol. 36, No. 2, 2005, pp. 91–106. doi:10.1016/j.fluiddyn.2004.12.002

[25] Yamaguchi, H., Zhang, X. R., Niu, X. D., and Yoshikawa, K., "Thermomagnetic Natural Convection of Thermo-Sensitive Magnetic Fluids in Cubic Cavity with Heat Generating Object Inside," *Journal of Magnetism and Magnetic Materials*, Vol. 322, No. 6, 2010, pp. 698–704. doi:10.1016/j.jmmm.2009.10.044

[26] Paroncini, M., and Corvaro, F., "Natural Convection in a Square Enclosure with a Hot Source," *International Journal of Thermal Sciences*, Vol. 48, No. 9, Sept. 2009, pp. 1683–1695. doi:10.1016/j.ijthermalsci.2009.02.005

[27] Manikonda, S., and Berz, M., "Multipole Expansion Solution of the Laplace Equation Using Surface Data, *Nuclear Instruments and*

*Methods in Physics Research Section A*, Vol. 558, No. 1, 2006, pp. 175–183.
doi:10.1016/j.nima.2005.11.081

[28] Sadat, H., and Prax C., "Application of the Diffuse Approximation for Solving Fluid Flow and Heat Transfer Problems," *International Journal of Heat and Mass Transfer*, Vol. 39, No. 1, Jan. 1996, pp. 214–218.
doi:10.1016/S0017-9310(96)85018-6

[29] Prax, C., Salagnac, P., and Sadat, H., "Diffuse Approximation and Control-Volume-Based Finite- Element Methods: A Comparative Study," *Numerical Heat Transfer*, Vol. 34, No. 3, Oct. 1998, pp. 303–321.
doi:10.1080/10407799808915060

[30] Prax, C., Sadat, H., and Salagnac, P., "Diffuse Approximation Method for Solving Natural Convection in Porous Media," *Transport in Porous Media*, Vol. 22, No. 2, Feb. 1996, pp. 215–223.
doi:10.1007/BF01143516

[31] Sadat, H., and Couturier, S., "Performance and Accuracy of a Meshless Method for Solving Laminar Natural Convection," *Numerical Heat Transfer*, Vol. 37, No. 4, 2000, pp. 455–467.
doi:10.1080/10407790050051146

[32] Sophy, T., Sadat, H., and Prax, C., "A Three Dimensional Formulation of a Meshless Method for Solving Fluid Flow and Heat Transfer Problems," *Numerical Heat Transfer*, Vol. 41, No. 5, 2002, pp. 433–445.
doi:10.1080/104077902753725894